ARTICLE

doi:10.1038/nature14863

Self-renewing diploid Axin2$^+$ cells fuel homeostatic renewal of the liver

Bruce Wang[1,2], Ludan Zhao[1], Matt Fish[1], Catriona Y. Logan[1] & Roel Nusse[1]

The source of new hepatocytes in the uninjured liver has remained an open question. By lineage tracing using the Wnt-responsive gene *Axin2* in mice, we identify a population of proliferating and self-renewing cells adjacent to the central vein in the liver lobule. These pericentral cells express the early liver progenitor marker Tbx3, are diploid, and thereby differ from mature hepatocytes, which are mostly polyploid. The descendants of pericentral cells differentiate into Tbx3-negative, polyploid hepatocytes, and can replace all hepatocytes along the liver lobule during homeostatic renewal. Adjacent central vein endothelial cells provide Wnt signals that maintain the pericentral cells, thereby constituting the niche. Thus, we identify a cell population in the liver that subserves homeostatic hepatocyte renewal, characterize its anatomical niche, and identify molecular signals that regulate its activity.

The cellular source of new hepatocytes in the adult liver and the molecular regulation of hepatocyte renewal are fundamental unanswered questions in liver biology. Recent studies in mice using genetic lineage tracing techniques have concluded that during homeostatic renewal, new hepatocytes arise by replication of pre-existing hepatocytes[1,2]. This is in line with the generally accepted view that in the uninjured state, hepatocyte homeostasis does not involve a stem cell population[3]. However, hepatocytes are heterogeneous, with striking differences in age and function across the liver lobule[4]. In addition, mature hepatocytes are generally polyploid (4N to 32N), a genomic state that compromises replicative capacity[5,6], posing limitations on possible contributions of these cells to long-term liver homeostasis. It has been unknown whether a specific subpopulation of cells serves homeostatic renewal in the liver, as happens in many other tissues[7–10].

Wnt proteins are secreted short-range signals that maintain stem cells in many adult mammalian tissues, and are produced by the specialized microenvironment referred to as the stem cell niche[11]. Wnt proteins signal primarily through the intracellular protein β-catenin to activate transcription. A universal transcriptional target of β-catenin-dependent Wnt signalling is Axin2, and its expression provides a reliable readout of cells responding to Wnt[11,12]. Genetic lineage tracing of Axin2$^+$ cells has identified stem cells in several adult mammalian tissues[10,13]. We have used this lineage tracing approach to identify a unique population of Wnt-responsive cells that surround the central vein. These diploid cells self-renew over the lifespan of the animal and progressively give rise to mature polyploid hepatocytes that can populate the entire liver lobule. We also show that these pericentral cells are maintained by Wnt-producing central vein endothelial cells that constitute the niche.

Axin2$^+$ pericentral cells generate expanding clones

In the adult liver, Axin2 is expressed in cells located around the central vein[14,15], which we confirmed by *in situ* hybridization (Fig. 1m). In order to mark and follow the fates of these Wnt-responsive cells, we used the tamoxifen-inducible Axin2-CreERT2;Rosa26-mTmG^{flox} mouse to pulse label Axin2$^+$ cells. In these experiments, a subset of Axin2$^+$ cells is labelled stochastically with membrane GFP after tamoxifen administration. The GFP label is permanent, allowing for fate mapping of initially labelled cells and their descendants[10,13]. A single low-dose of tamoxifen led to GFP labelling exclusively of pericentral hepatocytes (Fig. 1a). Control animals receiving corn oil did not show any GFP labelling (Extended Data Fig. 1). The GFP$^+$ cells expressed glutamine synthetase (GS), another known Wnt target gene[16] and a marker for pericentral hepatocytes (Fig. 1b). They were negative for carbamoyl-phosphate synthase 1 (CPS), which marks midlobular and periportal hepatocytes (Fig. 1c). Over time, the population of labelled cells expanded as large contiguous patches spreading directionally from the central vein towards the portal vein (Fig. 1d, g, j). One year after the marking, nearly all hepatocytes in some individual lobules were descendants of the initially labelled Axin2$^+$ cells (Fig. 1j), including hepatocytes that abut the portal vein (Fig. 1j, inset).

Pericentral cells that remained labelled throughout the course of the lineage trace maintained their distinct gene expression profile, expressing Axin2 (Extended Data Fig. 2) and GS (Fig. 1b, e, h, k) but not CPS (Fig. 1c, f, i, l). Conversely, the descendants of the labelled cells acquired different gene expression patterns as they moved away from the central vein. They lost Axin2 and GS expression and gained CPS expression suggesting that, as they move away from the pericentral region, they no longer receive Wnt signals (see below) and subsequently differentiate. Finally, throughout the lineage traces, all labelled cells expressed the hepatocyte marker HNF4α (Fig. 1n), but not markers of other liver cell types including biliary epithelial cells (data not shown), indicating that Axin2$^+$ cells contribute only to the hepatocyte lineage.

While Axin2$^+$ cells can generate all hepatocytes in a lobule over time, quantification of the labelling after one year showed that on average descendants of Axin2$^+$ cells replaced 30% of the area of the entire liver (Fig. 1o and Extended Data Fig. 3), accounting for approximately 40% of the hepatocytes.

Axin2$^+$ cells self-renew

A defining property of stem cells is the ability to self-renew. To test whether Axin2$^+$ cells self-renew, we labelled a maximum number of Axin2$^+$ cells by administering five consecutive daily doses of tamoxifen (Fig. 2a). Over time, the labelled cells expanded concentrically

[1]Department of Developmental Biology, Howard Hughes Medical Institute, Stanford Institute for Stem Cell Biology and Regenerative Medicine, Stanford University School of Medicine, Stanford, California 94305, USA. [2]Department of Medicine and Liver Center, University of California San Francisco, San Francisco, California 94143, USA.

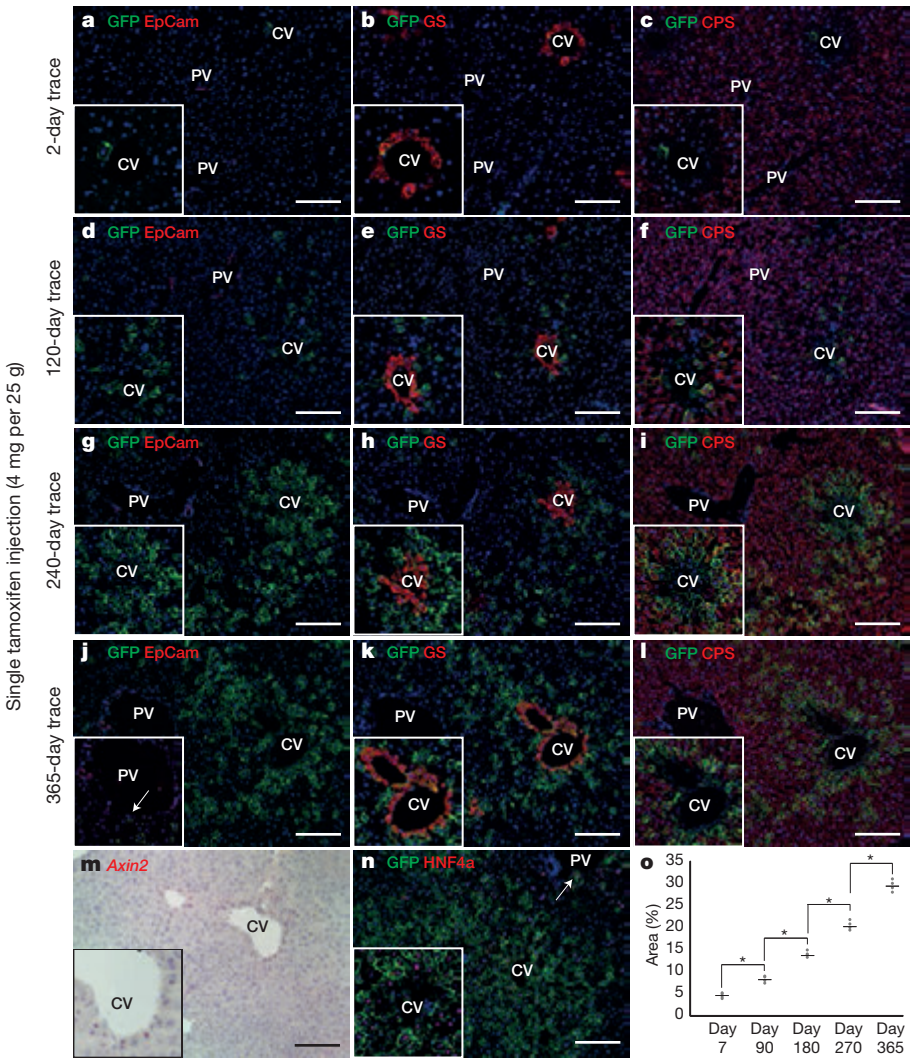

Figure 1 | Axin2$^+$ pericentral cells generate expanding clones of hepatocytes from the central vein towards the portal vein over time. **a**, Few pericentral hepatocytes are labelled in Axin2-CreERT2;Rosa26-mTmG^{flox} mice following a single dose of tamoxifen and traced for 2 days. EpCam labels bile ducts. **b**, **c**, Labelled pericentral cells express GS (**b**) but not CPS (**c**). **d**, **g**, **j**, The 120-day trace (**d**), 240-day trace (**g**) and 365-day trace (**j**) show expansion of labelled cells which can replace hepatocytes at the portal vein (**j** inset, arrow). **e**, **f**, **h**, **i**, **k**, **l**, Pericentral cells maintain GS expression (**e**, **h**, **k**), while labelled progeny acquire CPS expression (**f**, **i**, **l**). **m**, *In situ* hybridization for *Axin2*. **n**, All labelled cells express Hnf4a, including cells at the portal vein (arrow). **o**, Quantification of labelled hepatocytes over time. Data shows individual measurements and the mean. $n = 4$ animals for each time point. $^*P < 0.05$, two-tailed unpaired *t*-tests. CV, central vein; PV, portal vein. Scale bars, 100 μm.

from the central vein and, importantly, all pericentral cells remained labelled (Fig. 2b, c). This indicates that new pericentral cells arise exclusively from pre-existing labelled Axin2$^+$ cells. Thus, while Axin2$^+$ cells can give rise to all the hepatocytes along the lobule (Fig. 2c), they are not replaced by unlabelled Axin2$^-$ cells. That is, pericentral Axin2$^+$ cells are a self-renewing cell population.

To further characterize the Axin2$^+$ cell population, we used RNA-seq to compare the gene expression profile of FACS-isolated Axin2$^+$ and Axin2$^-$ hepatocytes (Extended Data Fig. 4). As expected, most of the differentially expressed genes between the two populations were known markers of liver zonation (Extended Data Table 1)[14,17]. However, we also identified *Tbx3*, a transcription factor important in maintaining pluripotency[18], as a gene upregulated in the Axin2$^+$ population. Notably, Tbx3 marks early hepatoblasts that arise around day 10 of embryogenesis, and is required for the earliest anlage of the liver[19]. By *in situ* hybridization, we confirmed that Tbx3 expression is uniquely expressed in the single layer of pericentral cells (Fig. 2d).

In Axin2-CreERT2 mice, one copy of the endogenous *Axin2* gene is inactivated. Since Axin2 is a negative feedback regulator of Wnt signalling[12], we considered the possibility that inactivation of one allele could confer a proliferative advantage after Wnt stimulation. To address this concern, we compared the DNA synthesis rate of Axin2$^+$ hepatocytes in wild-type versus Axin2-CreERT2$^{+/-}$ mice by 5-ethynyl-2′-deoxyuridine (EdU) incorporation. We used GS as the surrogate marker for Axin2$^+$ cells in wild-type animals because a suitable antibody for murine liver Axin2 staining does not exist. We found no difference in the DNA synthesis rate in the two strains of mice (Extended Data Fig. 5). We also controlled for the possibility of

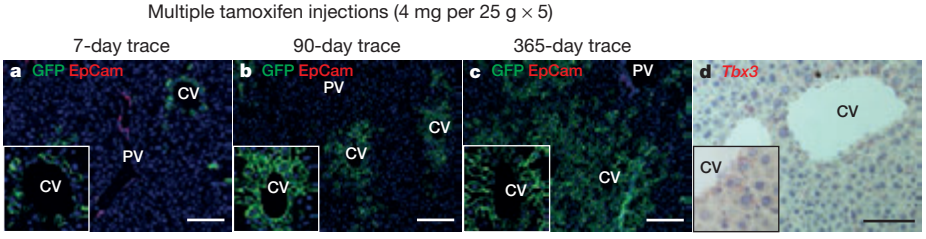

Figure 2 | Axin2$^+$ cells self-renew. **a**, The majority of pericentral hepatocytes are labelled in Axin2-CreERT2;Rosa26-mTmG^{flox} mice given five doses of tamoxifen and traced for 7 days. **b**, **c**, The 90-day trace (**b**) and 365-day trace (**c**) show that all pericentral cells remain labelled (see insets). Note that non-labelled cells do not occupy the pericentral region over time. **d**, *In situ* hybridization of *Tbx3*. CV, central vein; PV, portal vein. Scale bars, 100 μm.

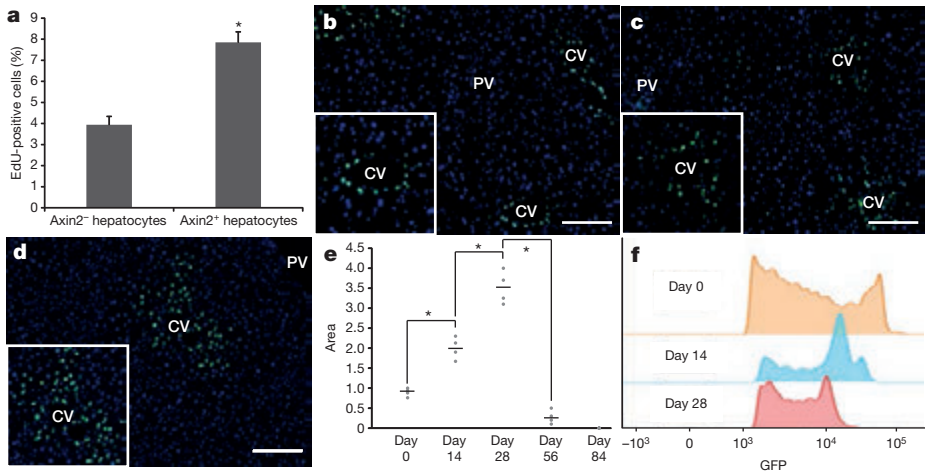

Figure 3 | Axin2$^+$ hepatocytes proliferate faster than other hepatocytes. **a**, Quantification of EdU$^+$ cells within Axin2$^-$ and Axin2$^+$ hepatocyte populations. Data represent mean ± s.e.m. $n = 5$ animals. $^*P < 0.05$, two-tailed unpaired *t*-test. **b**, All pericentral hepatocytes are labelled with nuclear GFP in Axin2-rtTA;TetO-H2B-GFP mice given doxycycline for 7 days. **c**, **d**, 14-day chase (**c**) and 28-day chase (**d**) after doxycycline. **e**, Quantification of GFP-labelled nuclei. Data shows individual measurements and the mean. $n = 4$ animals per group. $^*P < 0.05$, two-tailed unpaired *t*-tests. **f**, GFP intensity in day-0, day-14 and day-28 chase animals. Vertical axis shows number of events detected. CV, central vein; PV, portal vein. Scale bars, 100 μm.

liver injury from tamoxifen administration, which could serve as a proliferative stimulus[20]. We examined DNA synthesis by GS$^+$ pericentral hepatocytes in mice treated with corn oil or tamoxifen, comparing wild-type and Axin2-CreERT2$^{+/-}$ animals. We found no difference as measured by EdU incorporation (Extended Data Fig. 5). We conclude that neither *Axin2* gene dosage nor tamoxifen affects proliferation of Axin2$^+$ cells in our mouse model.

Axin2$^+$ cells proliferate faster than other hepatocytes

The fact that Axin2$^+$ cells repopulate most of the liver lobule over time implies a rate of proliferation that is greater than that of Axin2$^-$ hepatocytes. We quantified the DNA synthesis rates of the two cell populations as already described. Axin2-CreERT2;R26-mTmG^{flox} mice were labelled with tamoxifen and then given seven daily doses of EdU. We found that Axin2$^+$ cells undergo DNA replication twice as frequently as Axin2$^-$ hepatocytes (Fig. 3a).

To verify this result, we also examined the replicative activity of Axin2$^+$ cells by label dilution in which cells are tagged initially with a fixed amount of a stable product, which undergoes dilution with each cell division. We used the Axin2-rtTA;TetO-H2B-GFP transgenic mouse[21,22], which expresses a stable histone 2B–GFP fusion protein in Axin2$^+$ cells when given doxycycline. Additionally, the reverse tetracycline-controlled transactivator in Axin2-rtTA mice is under the control of a mouse Axin2 expression cassette[21], thus leaving the endogenous *Axin2* gene locus unaffected. Once activated by doxycycline, the H2B–GFP protein remains stably expressed until the labelled cell undergoes cell division, when the H2B–GFP protein is divided between the daughter cells, resulting in diminished GFP signal intensity[22].

Doxycycline was administered continuously for 7 days, at which time cells lining the central vein were labelled with nuclear GFP (Fig. 3b). Following a 14-day chase period after cessation of doxycycline, we observed that the number of GFP labelled cells had expanded, while the peak GFP signal intensity had decreased (Fig. 3c, f). The expansion of GFP-labelled cells around the central vein is concentric, consistent with the Axin2-CreERT2 lineage tracing results and is seen up to 28 days after cessation of doxycycline (Fig. 3d). By 56 days after cessation of doxycycline very few GFP-labelled cells are seen, and no labelled cells are observed after 84 days (Extended Data Fig. 6). We quantified the number of GFP$^+$ cells at each time point and found that the cell cycling rate is approximately every 14 days (Fig. 3e). We further confirmed this by FACS analysis, which showed step-wise dilution of the peak GFP signal intensity every 14 days (Fig. 3f). Thus, pericentral Axin2$^+$ cells actively proliferate during adult homeostasis, at an estimated cell cycling rate of 14 days.

Axin2$^+$ cells are mostly diploid

Mature hepatocytes are mostly polyploid[23], which is associated with decreased proliferative potential and increased senescence[6]. Stem cells are typically diploid, a property that may be necessary for unlimited duplication[24,25]. We used FACS sorting to isolate Axin2$^+$ cells and evaluated their ploidy status with Hoechst 33342 staining (Extended Data Fig. 7). As expected, the majority of unsorted hepatocytes are polyploid (Fig. 4a, c, left bar). In contrast, the majority of Axin2$^+$ cells are diploid (Fig. 4b, c, middle bar). To confirm that Axin2$^+$ diploid cells give rise to polyploid cells, we labelled Axin2$^+$ cells with tamoxifen, traced them for one year and isolated GFP$^+$ cells for ploidy analysis. We found that the ploidy distribution of the GFP$^+$ cells at the end of the trace was identical to that of unsorted hepatocytes (Fig. 4c, right bar), suggesting that the descendants of Axin2$^+$ cells mature normally into polyploid cells after leaving the pericentral zone.

Central vein endothelium acts as a Wnt-producing niche

The strict localization of Axin2$^+$ cells to the central vein suggested a local source of Wnt. We screened the normal liver for all nineteen mammalian Wnts by *in situ* hybridization[10]. Two of these, *Wnt2* and *Wnt9b*, were expressed exclusively in endothelial cells around the central vein (Fig. 5a, b), co-localizing with the endothelial cell marker *Pecam1* (Fig. 5c, d). We also isolated liver endothelial cells by FACS[26] and confirmed that both *Wnt2* and *Wnt9b* are highly expressed in endothelial cells by quantitative reverse-transcription PCR (Fig. 5e and Extended Data Fig. 8). Thus endothelial cells at the central vein produce *Wnt2* and *Wnt9b* as short-range signals for pericentral Axin2$^+$ cells and may constitute their niche.

Wnt signals are required for pericentral cell proliferation

The simultaneous and overlapping expression of two Wnt family members suggests functional redundancy of Wnt signalling at the central vein. To directly test whether endothelial-cell-derived Wnt proteins function to maintain the precursor state of pericentral cells, we conditionally deleted Wntless (*Wls*), a Wnt-specific transporter molecule required for proper Wnt protein secretion[27], specifically in endothelial cells. We crossed a VE-cadherin-CreERT2 mouse, which has a tamoxifen-inducible Cre-recombinase under the control of an endothelial cell specific promoter, with *Wls*$^{flox/flox}$ mice. Adult VE-cadherin-CreERT2;Wls$^{flox/flox}$ animals (Wls$^{f/f}$)[28,29] were given multiple

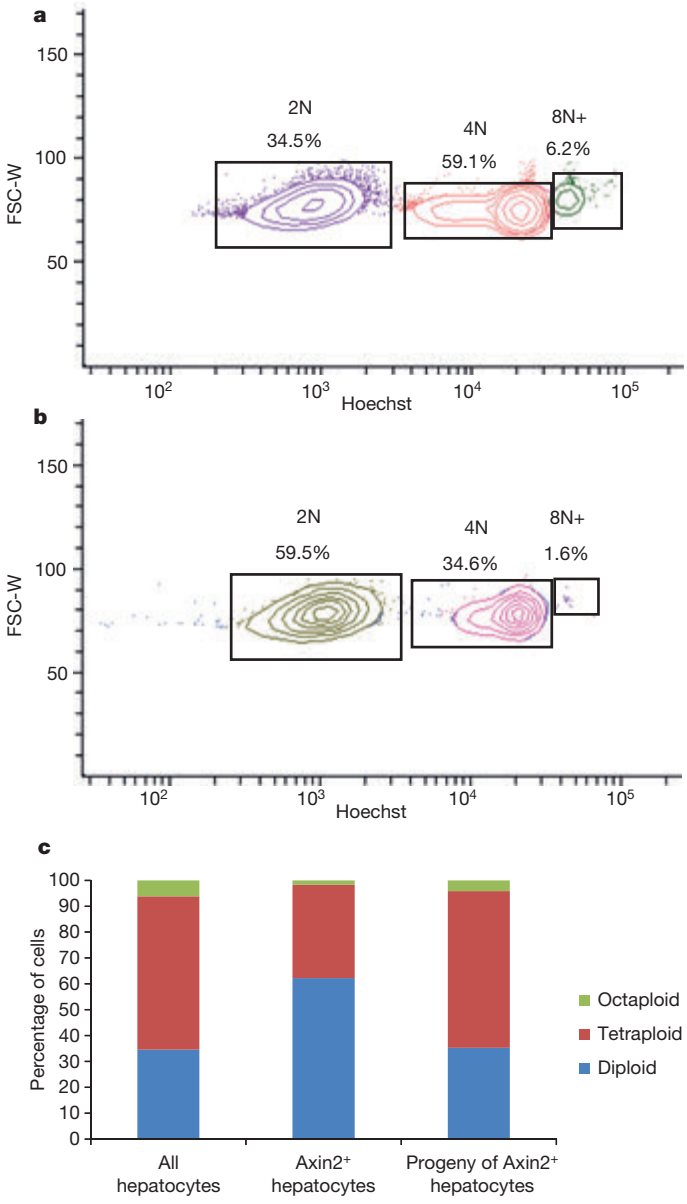

Figure 4 | Axin2$^+$ hepatocytes are mostly diploid. **a**, FACS plot of hepatocytes stained with Hoechst 33342 and gated for diploid (2N), tetraploid (4N) and octaploid or greater (8N+) cells. **b**, FACS plot of Axin2$^+$ hepatocytes stained with Hoechst 33342. FSC-W, forward scatter pulse width. **c**, Ploidy distribution within unsorted hepatocyte population (left), Axin2$^+$ hepatocyte population (centre), or labelled hepatocytes after lineage tracing for one year (right). $n = 3$ animals per group.

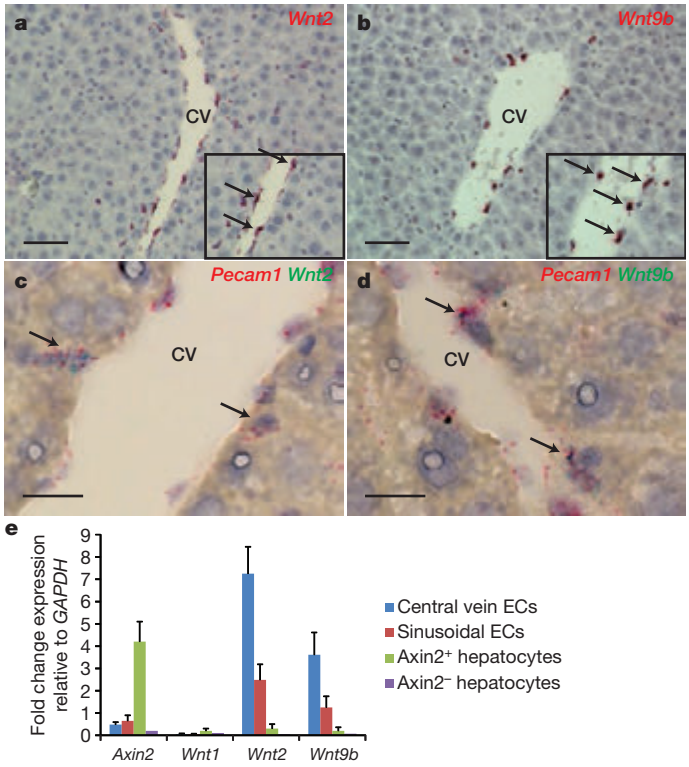

Figure 5 | Central vein endothelial cells produce Wnt proteins and act as a niche for pericentral cells. **a**, **b**, *In situ* hybridization of *Wnt2* (**a**) and *Wnt9b* (**b**) showing mRNA expression at the central vein in endothelial cells (arrows, inset). **c**, **d**, Co-*in situ* hybridization of *Pecam1* (red) and *Wnt2* (green) (**c**) and *Pecam1* and *Wnt9b* (**d**) showing co-expression in endothelial cells lining the central vein (arrows). **e**, Quantitative RT–PCR of *Axin2, Wnt1, Wnt2* and *Wnt9b* of FACS-isolated liver cells. EC, endothelial cells. Data represent mean ± s.e.m; $n = 5$ animals. Scale bars, 100 μm (**a**, **b**), 20 μm (**c**, **d**).

doses of tamoxifen to induce conditional deletion of Wls in endothelial cells. These mice appeared healthy without obvious systemic defects and their livers appeared grossly and histologically normal (Extended Data Fig. 9). Compared to VE-cadherin-CreERT2;Wls$^{flox/+}$ (Wls$^{f/+}$) control animals, *Axin2* expression was decreased in pericentral hepatocytes of Wls$^{f/f}$ mice (Fig. 6a–c), consistent with loss of Wnt signalling around the central vein. Concurrently, there was loss of pericentral hepatocyte function, as shown by significantly decreased levels of GS expression (Fig. 6d–f). Importantly, pericentral cells, labelled by GS, exhibited significantly decreased proliferation rates in Wls$^{f/f}$ mice compared to Wls$^{f/+}$ controls (Fig. 6g). The decreased rate approached the proliferation rate of GS$^-$ hepatocytes, though it remained significantly higher. This is probably due to the mosaic nature of tamoxifen-induced Wls inactivation. We conclude that endothelial-cell-derived Wnt signals are necessary for maintaining the high proliferative state of pericentral cells.

Discussion

In this paper we present a new view of hepatocyte homeostasis in the uninjured liver (Fig. 6h). We have identified a Wnt-responsive cell population that resides within a confined niche around the central vein. These cells self-renew and contribute to hepatocyte maintenance by differentiating into and replacing other hepatocytes along the hepatic lobule in the normal liver. The existence of this pericentral cell population suggests that the fundamental mechanisms regulating liver renewal are similar to other organs in which homeostatic renewal involves small populations of stem cells that maintain the tissue. In the liver however, our model is novel because it was previously thought that all hepatocytes are equivalent in their renewal potential. In contrast, we show that hepatocytes are made up of more than one cell type and are not equivalent in replicative ability during homeostasis. Given the properties of the cell population under study, we postulate that the Wnt-responsive pericentral cells are hepatocyte stem cells.

Several features make pericentral cells unique compared to other hepatocytes. Although pericentral cells express markers common to other hepatocytes, they also specifically express Axin2, Tbx3 and GS while lacking CPS. Pericentral cells proliferate at a higher rate compared to other hepatocytes, an observation that is consistent with ref. 30. Furthermore, pericentral cells possess a diploid genome, in contrast to most other hepatocytes, which are polyploid. Finally, and most importantly, while pericentral Axin2$^+$ cells can differentiate into all hepatocytes along the lobule, including those that line the portal vein, Axin2$^-$ hepatocytes do not replace pericentral cells during homeostasis. As pericentral cells can self-renew over the long term and differentiate into other hepatocytes, we suggest that they fit the functional definition of a stem cell.

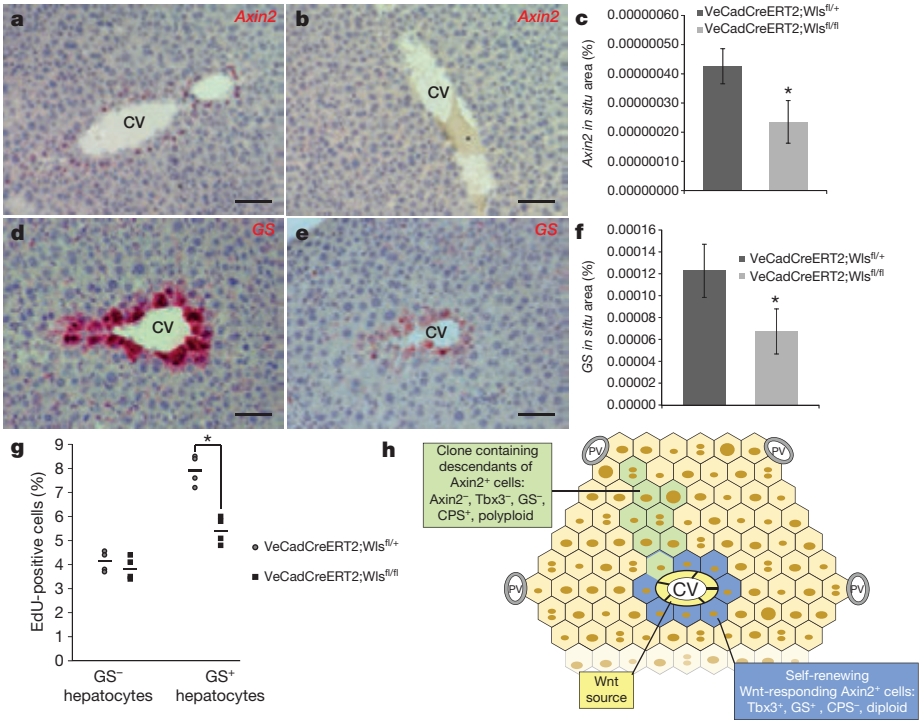

Figure 6 | Central-vein-derived Wnt proteins are required for pericentral cell proliferation. **a**, **b**, *Axin2 in situ* hybridization in $Wls^{f/+}$ (**a**), and $Wls^{f/f}$ (**b**) mice. **c**, Quantification of *Axin2 in situ* signal. Data represent mean ± s.e.m.; $n = 5$ animals per group. $^*P < 0.05$, two-tailed unpaired *t*-test. **d**, **e**, *GS in situ* hybridization in $Wls^{f/+}$ (**d**) and $Wls^{f/f}$ (**e**) mice. **f**, Quantification of *GS in situ* signal. Data represent mean ± s.e.m.; $n = 5$ animals per group. $^*P < 0.05$, two-tailed unpaired *t*-test. **g**, Quantification of EdU^+ cells within GS^- or GS^+ hepatocyte populations in $Wls^{fl/+}$ and $Wls^{fl/fl}$ animals. Data shows individual measurements and the mean. $n = 4$ animals per group. $^*P < 0.05$, two-tailed unpaired *t*-test. **h**, Schematic of hepatocyte homeostatic renewal by pericentral cells. CV, central vein; PV, portal vein. Scale bars, 100 μm.

The diploid nature of pericentral cells is important and surprising, although nuclear size measurements in rat livers have suggested the presence of smaller nuclei near the central vein[31]. This sheds light on a long-standing question in liver biology. Mature polyploid hepatocytes display chromosomal abnormalities[5,32] and display impaired replication[5,6]. By maintaining a diploid genome, the pericentral cells would, like stem cells[25], retain unlimited replicative potential. It is interesting to note that during the cell cycle, levels of Wnt signalling peak at the G2/M phase[33]. If Wnt proteins regulate expression of mitotic control genes such as the phosphatase *Cdc25*[34], they could direct cells to mitosis and continued diploidy rather than to non-mitotic DNA replication and polyploidy.

A defining feature of pericentral cells is their localization to a Wnt-rich anatomical niche. While Wnt-regulated genes such as β-catenin and *Apc* are known to function in liver development[35] and zonation[14], the types and sources of Wnt have not been identified. We found that Wnt9b is specifically expressed in endothelial cells at the central vein, adjacent to the pericentral cells, while Wnt2 is expressed in both the sinusoidal and central vein endothelial cells. Notably, Wnt2 produced by sinusoidal endothelial cells is known to be important for hepatocyte regeneration after injury[26]. Similarly, in other stem cell niches, lipid-modified Wnt signals act as short-range cues, maintaining stem cells in the immediate vicinity of the niche but not outside[11].

It has been suggested that there may be a periportal source of new hepatocytes under normal conditions[36]. Our lineage tracing studies do not exclude the possibility that other sources of hepatocytes exist during homeostasis since after one year the descendants of pericentral cells replace on average only 40% of hepatocytes within the liver. However, a portal-based population would be regulated differently, since we find no expression of Wnt9b by the portal vein endothelium.

Liver is known to regenerate efficiently after injuries such as partial hepatectomy or chemical insult. It has been reported that during regeneration after chemical damage, a Wnt-responsive population of cells near the portal vein can be labelled by the *Lgr5* receptor gene[15]. These cells, unlike pericentral $Axin2^+$ cells, do not express hepatocyte genes, but subsequently differentiate into bile duct epithelial cells and hepatocytes and thus could be similar to injury-induced oval cells[3]. Clearly, $Lgr5^+$/oval cells are distinct from the cells we identify here, as pericentral cells maintain hepatocyte homeostasis in the uninjured liver while $Lgr5^+$/oval cells have only been reported after injury.

The stem cell marker Tbx3 is expressed widely in early liver hepatoblasts and is important for hepatoblast proliferation and initiation of hepatocyte differentiation[19,37]. Our findings that pericentral cells also express Tbx3 leads to the intriguing hypothesis that pericentral cells may represent the persistence of an embryonic hepatocyte progenitor population into a self-renewing cell population in the mature liver.

It is noteworthy that liver cancer is often characterized by loss-of-function mutations in negative regulators of the Wnt pathway, including Axin and APC[38]. In a mouse model of liver cancer caused by Met overexpression, liver tumours were found to arise exclusively from cells located at the central vein[39,40], suggesting that pericentral $Axin2^+$ cells, normally controlled by a paracrine Wnt signal, are precursors to liver cancer. This would explain why liver tumours contain mostly diploid cells[41], an observation that was earlier rationalized by polyploid hepatocytes becoming diploid after oncogenic transformation.

Online Content Methods, along with any additional Extended Data display items and Source Data, are available in the online version of the paper; references unique to these sections appear only in the online paper.

Received 19 November 2014; accepted 29 June 2015.
Published online 5 August 2015.

1. Malato, Y. *et al.* Fate tracing of mature hepatocytes in mouse liver homeostasis and regeneration. *J. Clin. Invest.* **121,** 4850–4860 (2011).
2. Yanger, K. *et al.* Adult hepatocytes are generated by self-duplication rather than stem cell differentiation. *Cell Stem Cell* **15,** 340–349 (2014).

3. Miyajima, A., Tanaka, M. & Itoh, T. Stem/progenitor cells in liver development, homeostasis, regeneration, and reprogramming. *Cell Stem Cell* **14,** 561–574 (2014).
4. Jungermann, K. & Kietzmann, T. Zonation of parenchymal and nonparenchymal metabolism in liver. *Annu. Rev. Nutr.* **16,** 179–203 (1996).
5. Ganem, N. J. & Pellman, D. Limiting the proliferation of polyploid cells. *Cell* **131,** 437–440 (2007).
6. Sigal, S. H. *et al.* Partial hepatectomy-induced polyploidy attenuates hepatocyte replication and activates cell aging events. *Am. J. Physiol.* **276,** G1260–G1272 (1999).
7. DasGupta, R. & Fuchs, E. Multiple roles for activated LEF/TCF transcription complexes during hair follicle development and differentiation. *Development* **126,** 4557–4568 (1999).
8. Zeng, Y. A. & Nusse, R. Wnt proteins are self-renewal factors for mammary stem cells and promote their long-term expansion in culture. *Cell Stem Cell* **6,** 568–577 (2010).
9. Barker, N. *et al.* Identification of stem cells in small intestine and colon by marker gene *Lgr5*. *Nature* **449,** 1003–1007 (2007).
10. Lim, X. *et al.* Interfollicular epidermal stem cells self-renew via autocrine Wnt signaling. *Science* **342,** 1226–1230 (2013).
11. Clevers, H., Loh, K. M. & Nusse, R. Stem cell signaling. An integral program for tissue renewal and regeneration: Wnt signaling and stem cell control. *Science* **346,** 1248012 (2014).
12. Lustig, B. *et al.* Negative feedback loop of Wnt signaling through upregulation of conductin/axin2 in colorectal and liver tumors. *Mol. Cell. Biol.* **22,** 1184–1193 (2002).
13. van Amerongen, R., Bowman, A. N. & Nusse, R. Developmental stage and time dictate the fate of Wnt/β-catenin-responsive stem cells in the mammary gland. *Cell Stem Cell* **11,** 387–400 (2012).
14. Benhamouche, S. *et al. Apc* tumor suppressor gene is the ''zonation-keeper'' of mouse liver. *Dev. Cell* **10,** 759–770 (2006).
15. Huch, M. *et al. In vitro* expansion of single $Lgr5^{+}$ liver stem cells induced by Wnt-driven regeneration. *Nature* **494,** 247–250 (2013).
16. Cadoret, A. *et al.* New targets of β-catenin signaling in the liver are involved in the glutamine metabolism. *Oncogene* **21,** 8293–8301 (2002).
17. Braeuning, A. *et al.* Differential gene expression in periportal and perivenous mouse hepatocytes. *FEBS J.* **273,** 5051–5061 (2006).
18. Han, J. *et al.* Tbx3 improves the germ-line competency of induced pluripotent stem cells. *Nature* **463,** 1096–1100 (2010).
19. Suzuki, A. *et al.* Tbx3 controls the fate of hepatic progenitor cells in liver development by suppressing p19ARF expression. *Development* **135,** 1589–1595 (2008).
20. Moreira, P. I. *et al.* Estradiol affects liver mitochondrial function in ovariectomized and tamoxifen-treated ovariectomized female rats. *Toxicol. Appl. Pharmacol.* **221,** 102–110 (2007).
21. Yu, H. M. *et al.* Impaired neural development caused by inducible expression of Axin in transgenic mice. *Mech. Dev.* **124,** 146–156 (2007).
22. Tumbar, T. Defining the epithelial stem cell niche in skin. *Science* **303,** 359–363 (2004).
23. Guidotti, J. E. *et al.* Liver cell polyploidization: a pivotal role for binuclear hepatocytes. *J. Biol. Chem.* **278,** 19095–19101 (2003).
24. Comai, L. The advantages and disadvantages of being polyploid. *Nature Rev. Genet.* **6,** 836–846 (2005).
25. Ohlstein, B., &. Spradling, A. The adult *Drosophila* posterior midgut is maintained by pluripotent stem cells. *Nature* **439,** 470–474 (2006).
26. Ding, B.-S. *et al.* Inductive angiocrine signals from sinusoidal endothelium are required for liver regeneration. *Nature* **468,** 310–315 (2010).
27. Bänziger, C. *et al.* Wntless, a conserved membrane protein dedicated to the secretion of Wnt proteins from signaling cells. *Cell* **125,** 509–522 (2006).
28. Monvoisin, A. *et al.* VE-cadherin-$CreER^{T2}$ transgenic mouse: a model for inducible recombination in the endothelium. *Dev. Dyn.* **235,** 3413–3422 (2006).
29. Carpenter, A. C. *et al.* Generation of mice with a conditional null allele for Wntless. *Genesis* **48,** 554–558 (2010).
30. Magami, Y. *et al.* Cell proliferation and renewal of normal hepatocytes and bile duct cells in adult mouse liver. *Liver* **22,** 419–425 (2002).
31. Zajicek, G. & Schwartz-Arad, D. Streaming liver VII: DNA turnover in acinus zone-3. *Liver* **10,** 137–140 (1990).
32. Duncan, A. W. *et al.* The ploidy conveyor of mature hepatocytes as a source of genetic variation. *Nature* **467,** 707–710 (2010).
33. Niehrs, C. & Acebron, S. P. Mitotic and mitogenic Wnt signalling. *EMBO J.* **31,** 2705–2713 (2012).
34. Vijayakumar, S. *et al.* High-frequency canonical Wnt activation in multiple sarcoma subtypes drives proliferation through a TCF/β-catenin target gene, CDC25A. *Cancer Cell* **19,** 601–612 (2011).
35. Tan, X. *et al.* β-Catenin deletion in hepatoblasts disrupts hepatic morphogenesis and survival during mouse development. *Hepatology* **47,** 1667–1679 (2008).
36. Zajicek, G., Oren, R. & Weinreb, M. Jr. The streaming liver. *Liver* **5,** 293–300 (1985).
37. Lüdtke, T. H. *et al.* Tbx3 promotes liver bud expansion during mouse development by suppression of cholangiocyte differentiation. *Hepatology* **49,** 969–978 (2009).
38. Laurent-Puig, P. & Zucman-Rossi, J. Genetics of hepatocellular tumors. *Oncogene* **25,** 3778–3786 (2006).
39. Wang, R. *et al.* Activation of the Met receptor by cell attachment induces and sustains hepatocellular carcinomas in transgenic mice. *J. Cell Biol.* **153,** 1023–1034 (2001).
40. Tward, A. D. *et al.* Distinct pathways of genomic progression to benign and malignant tumors of the liver. *Proc. Natl Acad. Sci. USA* **104,** 14771–14776 (2007).
41. Schwarze, P. E. *et al.* Emergence of a population of small, diploid hepatocytes during hepatocarcinogenesis. *Carcinogenesis* **5,** 1267–1275 (1984).

Supplementary Information is available in the online version of the paper.

Acknowledgements These studies were supported by the Howard Hughes Medical Institute and a grant from the Reed-Stinehart foundation. R.N. is an investigator with the Howard Hughes Medical Institute. B.W. was supported by F32DK091005. We thank D. M. Bissell and T. Desai for comments on the manuscript, V. Waehle for assistance in preparing RNA samples for RNA-seq, M. Britton for RNA-seq analysis, and P. Lovelace for assistance with FACS.

Author Contributions B.W. carried out the experiments. D.Z. performed qRT–PCR analysis. M.F. performed *in situ* hybridization. C.Y.L. performed RNA-seq analysis. B.W. and R.N. designed the study, analysed data and wrote the paper. All authors discussed the results and commented on the manuscript.

Author Information The data discussed in this publication have been deposited in NCBI's Gene Expression Omnibus and are accessible through GEO Series accession number GSE68806. Reprints and permissions information is available at www.nature.com/reprints. The authors declare no competing financial interests. Readers are welcome to comment on the online version of the paper. Correspondence and requests for materials should be addressed to R.N. (rnusse@stanford.edu) and B.W. (bruce.wang@ucsf.edu).

METHODS

Animals. B6 and FVB mice (Charles River Laboratories) were used for wild-type analysis. Axin2-CreERT2 mice[13] and VE-cadherin-CreERT2 mice[28] have been previously described. Rosa26-mTmG^{flox} (*Gt(ROSA)26Sor*$^{tm4(ACTB-tdTomato,-EGFP)Luo}$/J)[42], Wls^{flox} (129S-*Wls*$^{tm1.1Lan}$/J)[29], Axin2-rtTA (B6.Cg-Tg(Axin2-rtTA2S*M2)7Cos/J)[21], and TetO-H2B-GFP (Tg(tetO-HIST1H2BJ/GFP)47Efu/J)[22] mice were obtained from The Jackson Laboratory. All alleles were heterozygous, except where stated.

For lineage tracing studies, Axin2-CreERT2;Rosa26-mTmG^{flox} mice 8–12 weeks of age received intraperitoneal injections of tamoxifen (Sigma, 4 mg per 25 g mouse weight) dissolved in 10% ethanol/corn oil (Sigma) either once or on five consecutive days. Representative figures of Axin2-CreERT2;Rosa26-mTmG^{flox} lineage tracing (Figs 1a–l and 2a–c) are from $n = 5$ animals per time point. Quantification of the area of labelled hepatocytes (Fig. 1o) was performed on Axin2-CreERT2/Rosa26-mTmG^{flox} mice given five daily doses of tamoxifen and lineage traced.

For label dilution studies Axin2-rtTA;TetO-H2B-GFP mice 8–12 weeks old received doxycycline hyclate (Sigma, 1 mg ml^{-1}) in drinking water for 7 days, then chased for 0, 14, 28, 56 or 84 days. Representative figures of Axin2rtTA; TetO-H2B-GFP label dilution (Fig. 3b–d) are from $n = 4$ animals per time point.

For the endothelial cell conditional knockout of Wntless, VE-cadherin-CreERT2;Wls^{flox} mice (Wls$^{f/f}$ and Wls$^{f/+}$) aged 8–10 weeks received intraperitoneal injections of tamoxifen on five consecutive days and sacrificed 7 days after the last dose of tamoxifen. For proliferation studies (Fig. 6g), mice were given seven consecutive daily doses of EdU after the last dose of tamoxifen and sacrificed 2 h after the last EdU dose.

All animal experiments and methods were approved by the Institutional Animal Care and Use Committee at Stanford University. Mice used in this study were age- and gender-matched littermates including both sexes. All mice were housed in the animal facility of Stanford University on a 12-h light/dark cycle with *ad libitum* access to water and normal chow except when otherwise indicated. The animal experiments were not randomized. The investigators were not blinded to allocation during experiments and outcome assessment.

Statistics. The statistical analysis used to measure significance is the two-tailed unpaired Student's *t*-test. The G*Power calculator (G*Power 3.1.9.2) was used for sample size calculations. For an α probability of 0.05, a β probability of 0.8, expected observed differences between the two comparison groups of 50% and assuming 15% standard error of the mean within each group, the sample size required to detect a statistically significant difference is four animals per group.

Liver histology and immunofluorescence. Mouse livers were fixed in 4% PFA overnight at 4 °C, cryoprotected in 30% sucrose for 24 h at 4 °C then embedded in OCT and snap frozen. All immunofluorescence staining was performed in the dark. Cryosections (10 µm) were incubated in blocking buffer (5% normal donkey serum, 0.5% Triton-X in PBS) at room temperature and stained with primary and secondary antibodies, then mounted in Prolong Gold with DAPI mounting medium (Life Technologies). The following primary antibodies were used: GFP (chicken, 1:500, Abcam ab13970), GS (mouse, 1:500, Millipore MAB302), CPS (rabbit, 1:100, gift from W. Lamers), EpCAM (rabbit, 1:100, Developmental Studies Hybridoma Bank, clone g8.8), HNF4α (rabbit, 1:100, Santa Cruz Biotechnology sc-8987).

Hepatocyte proliferation assay. Hepatocyte proliferation *in vivo* was measured by 5-ethynyl-2′-deoxyuridine (EdU) uptake. In brief, mice received a dose of intraperitoneal EdU (Life Technologies, 50 mg per kg mouse weight) daily for 7 days and harvested half a day after the final EdU dose. For EdU detection, cryosections were first stained with the appropriated primary and secondary antibodies, then incubated with the reagents in the Click-iT EdU Alexa Fluor 555 Imaging Kit (Life Technologies) prepared according to the manufacturer's instructions and mounted in Prolong Gold with DAPI mounting medium.

Liver cell isolation and flow cytometry. Hepatocytes and liver endothelial cells were isolated from mice by a two-step collagenase perfusion technique with modifications. In brief, after the inferior vena cava was cannulated and portal vein was cut, the liver was perfused at 10 ml min^{-1} through the inferior vena cava with Liver Perfusion Medium (Invitrogen) at 37 °C for 10 min, followed by perfusion with collagenase type IV (Wellington) for an additional 10 min. The liver was dissociated and passed through a 70 µm filter. Hepatocytes were separated from non-parenchymal cells (NPCs) by low-speed centrifugation (30*g* for 3 min × 3), and further purified by Percoll gradient centrifugation as previously described[43]. NPCs were pelleted from supernatant by centrifugation (300*g* for 5 min × 3) and then stained with cell surface markers for endothelial cell isolation and flow cytometric analysis as previously described[26].

Cells were analysed on FACS ARIA II (BD). Data were processed with FACSDiva 8.0 software (BD) and FlowJo v10 (FlowJo). Doublets were excluded by FSC-W × FSC-H and SSC-W × SSC-H analysis. Single-stained channels were used for compensation and fluorophore minus one controls were used for gating. The following antibodies were used: CD31-PE (eBioscience 12-0311-81), CD34-FITC (eBioscience 11-0341-85), rat VEGFR3 (gift from B.-S. Ding) with anti-rat Alexa Fluor 647 secondary (Jackson Immuno 712-605-153). Sinusoidal endothelial cells were identified as VEGFR3$^+$CD31$^+$CD34$^-$ cells. Central vein endothelial cells were identified as VEGFR3$^-$CD31$^+$CD34$^+$ cells.

Hepatocyte ploidy measurement. Hepatocyte ploidy staining was performed as previously described[32]. Wild-type FVB mice were used for baseline hepatocyte ploidy measurements. For ploidy measurement of Axin2$^+$ hepatocytes, Axin2-CreERT2;Rosa26-mTmG^{flox} mice were given five daily doses of tamoxifen (4 mg per 25 g body weight) and cells were isolated 2 days or 1 year after the last dose of tamoxifen and stained with Hoechst 33342 (Invitrogen). Cells were analysed on FACS ARIA II (BD). Data were processed with FACSDiva 8.0 software (BD) and FlowJo v10. FACS plots (Fig. 4a, b) are representative ploidy plots from $n = 5$ wild-type animals and $n = 3$ Axin2-CreERT2;Rosa26-mTmG^{flox} mice, respectively.

Real-time RT–PCR analysis. Liver endothelial cells were FACS sorted as described above. Cells were homogenized using QIAshredder (Qiagen) and total RNA was purified using an RNeasy mini kit (Qiagen) according to the manufacturer's instructions. The total RNA was reverse transcribed using random primers (High Capacity cDNA Reverse Transcription kit, Life Technologies). Gene expression was then assayed by real-time PCR using TaqMan Gene Expression Assays (Applied Biosystems) on an ABI 7900HT real-time PCR system. The following TaqMan probes were used: *Axin2* (Mm00443610), *Wnt1* (Mm01300555), *Wnt2* (Mm00470018), *Wnt9b* (Mm00457102).

RNAscope *in situ* hybridization. Paraffin-embedded liver sections (5 µm) were processed for RNA *in situ* detection using the RNAscope 2-plex Detection Kit (Chromogenic) according to the manufacturer's instructions (Advanced Cell Diagnostics)[43]. RNAscope probes used were: *Axin2* (NM 015732, region 330-1287), *GS* (NM 008131, region 103-973), *Wnt2* (NM 023653, region 857-2086), *Wnt9b* (NM 011719, region 727-1616), *PECAM1* (NM 001032378, region 915-1827), Tbx3 (NM 198052).

Representative figures of *in situ* hybridization of *Tbx3* (Fig. 2d), *Wnt2, Wnt9b* and *Pecam1* (Fig. 5a–d) are from $n = 5$ wild-type B6 mice aged 8 weeks.

Representative figures of *in situ* hybridization from VE-cadherin-CreERT2; Wls^{flox} studies (Fig. 6a, b, d, e) are from $n = 5$ mice from each group.

Microscope image acquisition and quantification. All sections were imaged using the Axioplan 2 microscope, the AxioCam MRm (fluorescence) and MRC5 (bright field) cameras and using Axiovision AC software (Release 4.8, Carl Zeiss). Image acquisitions were done at room temperature using ×10 NA 0.3, ×20 NA 0.5, and ×40 NA 0.75 EC Plan-Neofluar objectives. Co-localization images were obtained using confocal microscopy using a Leica SP5 confocal detection system fitted on a Leica DMI6000 inverted microscope equipped with a ×20 NA 0.75 HC PL apochromatic glycerol-immersion objective, and a ×40 NA 1.3 HCX PL apochromatic oil-immersion objective (Leica) and using Leica LAS AF system software. For fluorescence area quantification, tiled images of entire liver sections were acquired using a Zeiss Cell Observer Spinning Disc confocal system on an Axio Observer.Z1 inverted microscope with Zen 2012 software (blue edition). Image acquisitions were done at room temperature using a ×20 NA 0.5 EC Plan-Neofluar objective.

Tiled images were stitched together in Zen 2012 (blue edition) and quantified using ImageJ. For some images, contrast, colour and dynamic range were globally adjusted in Adobe Photoshop (Adobe Systems). Nuclei for EdU-labelled and total cell counts were quantified using ImageJ. Thresholding and watershed transforms were used. Pericentral hepatocytes were identified with either GFP (in Axin2-CreERT2;Rosa26-mTmG^{flox} mice) or GS (in wild-type or VE-cadherin-CreERT2;Wls^{flox} mice). GFP$^+$ and GS$^+$ cells were quantified manually. Axin2 and GS *in situ* images were quantified with RNAscope SpotStudio software (version 1.0, Advanced Cell Diagnostics)[44].

RNA-seq analysis. Using hepatocytes isolated from Axin2-rtTA;TetO-H2B-GFP animals, GFP$^+$ and GFP$^-$ cells from three animals were sorted using FACS. Cells were lysed in TRIzol (Life Technologies) and treated with chloroform. The aqueous layer was precipitated with ethanol and RNA was isolated with QIAGEN RNAeasy Mini kit following the manufacturer's instructions. cDNA barcoded libraries were made using the TruSeq Stranded mRNA Sample Prep Kit (Illumina) following the manufacturer's instructions. Samples were sequenced on an Illumina HiSeq 2000 instrument (three samples per lane, 100-bp paired-end reads) to yield>50 million reads per sample.

Processing and analysis of FASTQ files were performed using Galaxy[45]. A custom Galaxy instance (UC Davis Bioinformatics Core) was run on Amazon AWS. Removal of adaptor contamination and quality trimming were performed using Scythe v1.21 (https://github.com/ucdavis-bioinformatics/scythe) and Sickle v1.21 (https://github.com/ucdavis-bioinformatics/sickle). TopHat v2.0.11[46] was

used to align reads to the mouse mm10 assembly, and Cuffdiff v.2.2.2[47] was used for differential gene expression analysis.

The data discussed in this publication have been deposited in NCBI's Gene Expression Omnibus[48] and are accessible through GEO Series accession number GSE68806.

42. Muzumdar, M. D. *et al.* A global double-fluorescent Cre reporter mouse. *Genesis* **45,** 593–605 (2007).
43. Kreamer, B. L. *et al.* Use of a low-speed, iso-density percoll centrifugation method to increase the viability of isolated rat hepatocyte preparations. *In Vitro Cell. Dev. Biol.* **22,** 201–211 (1986).
44. Wang, F. *et al.* RNAscope: a novel *in situ* RNA analysis platform for formalin-fixed, paraffin-embedded tissues. *J. Mol. Diagn.* **14,** 22–29 (2012).
45. Goecks, J. *et al.* Galaxy: a comprehensive approach for supporting accessible, reproducible, and transparent computational research in the life sciences. *Genome Biol.* **11,** R86 (2010).
46. Kim, D. *et al.* TopHat2: accurate alignment of transcriptomes in the presence of insertions, deletions and gene fusions. *Genome Biol.* **14,** R36 (2013).
47. Trapnell, C. *et al.* Differential analysis of gene regulation at transcript resolution with RNA-seq. *Nature Biotechnol.* **31,** 46–53 (2013).
48. Edgar, R., Domrachev, M. & Lash, A. E. Gene Expression Omnibus: NCBI gene expression and hybridization array data repository. *Nucleic Acids Res.* **30,** 207–210 (2002).

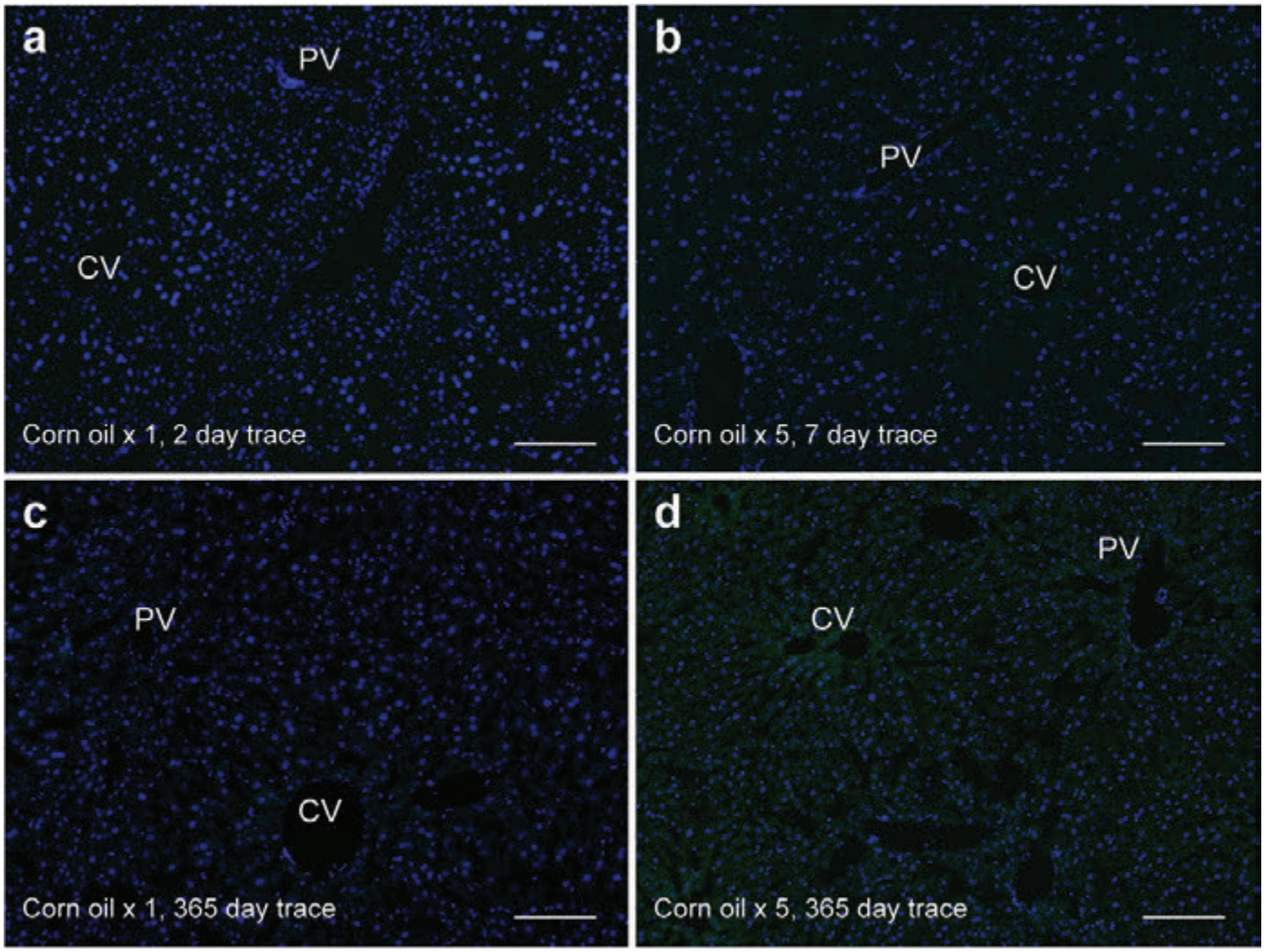

Extended Data Figure 1 | Leakiness in Axin2-CreERT2;Rosa26-mTmG^{flox} mice is not observed in animals injected with corn oil. **a**, **c**, No GFP labelling is seen in Axin2-CreERT2;Rosa26-mTmG^{flox} mice after a single dose of corn oil and traced for 2 days (**a**) or 365 days (**c**). **b**, **d**, No GFP labelling is seen after five consecutive daily doses of corn oil and traced for 7 days (**b**) or 365 days (**d**). All animals were 8-week-old Axin2-CreERT2;Rosa26-mTmG^{flox} mice. Images are representative images from $n = 5$ mice per condition and time point. CV, central vein; PV, portal vein. Scale bars, 100 µm.

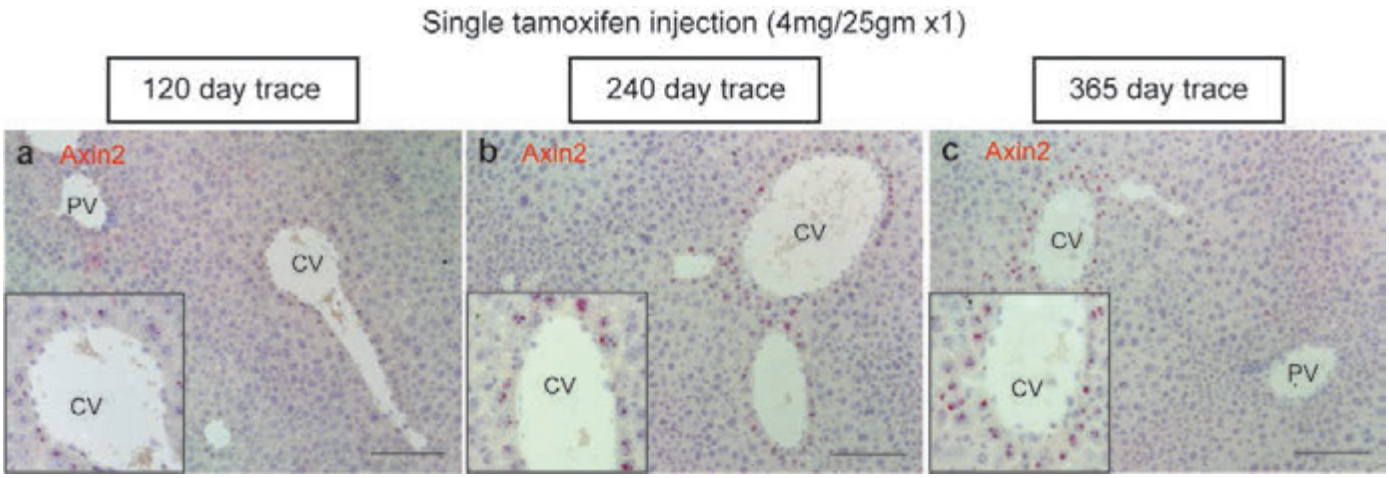

Extended Data Figure 2 | Axin2 expression remains restricted to pericentral cells. **a**–**c**, *In situ* hybridization for *Axin2* in 120-day trace (**a**), 240-day trace (**b**) and 365-day trace (**c**) Axin2-CreERT2;Rosa26-mTmG^{flox} mice. Representative *in situ* images are from $n = 5$ animals per time point. CV, central vein; PV, portal vein. Scale bars, 100 μm.

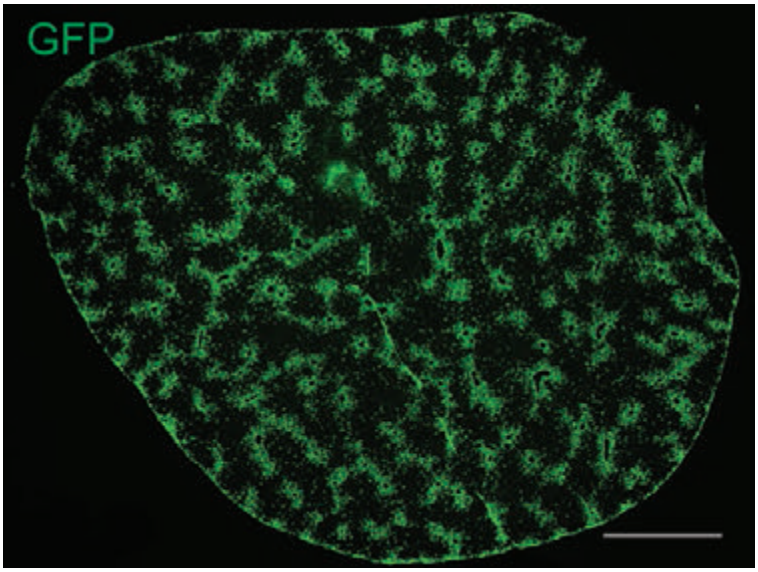

Extended Data Figure 3 | Descendants of Axin2^{+} cells replaced 30% of the area of the liver. Tiled image of entire liver section of a 365-day trace Axin2-CreERT2;Rosa26-mTmG^{flox} mice. Image is representative of $n = 5$ animals at this time point. Scale bar, 2,500 μm.

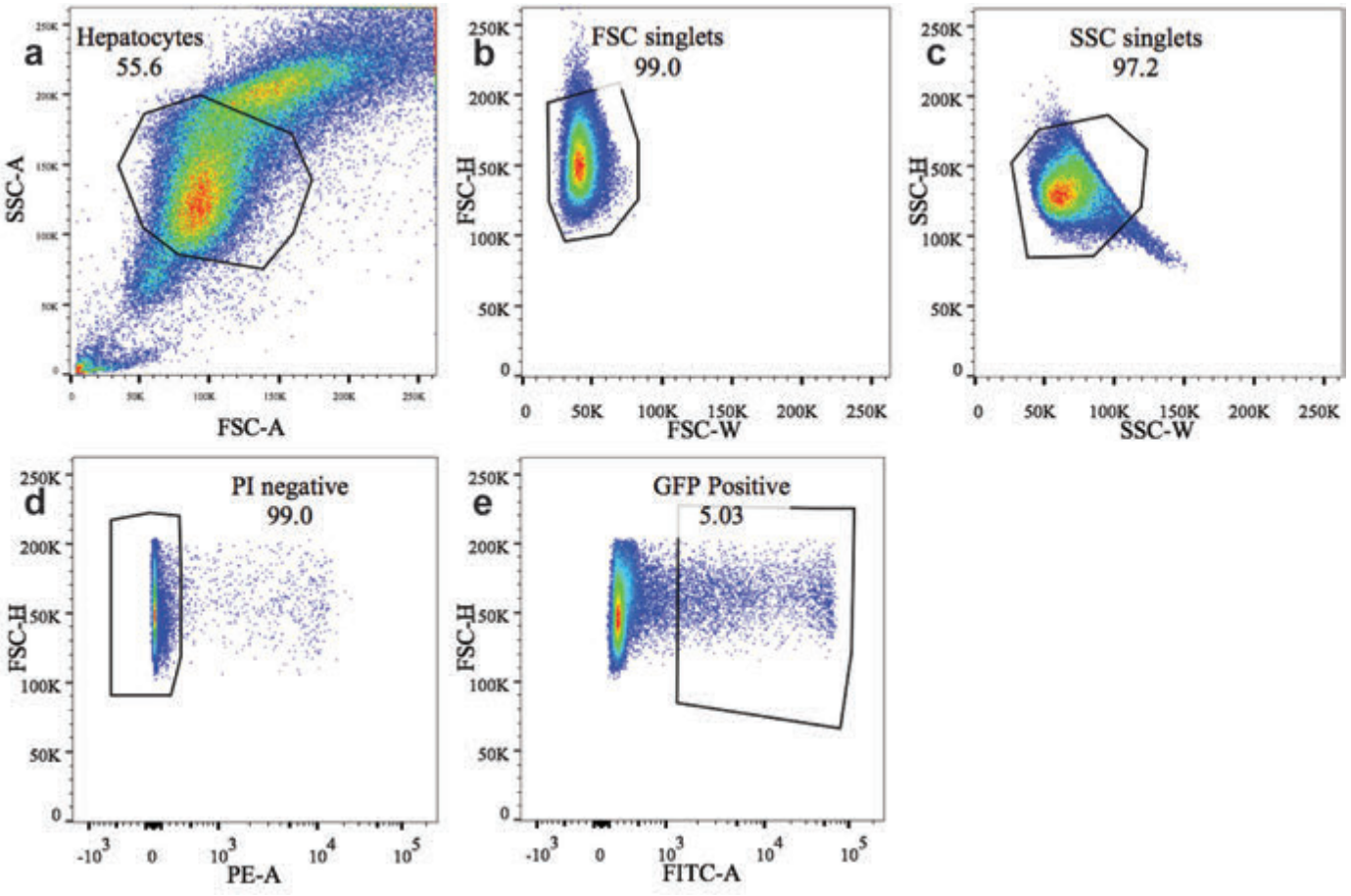

Extended Data Figure 4 | FACS sorting gates for GFP$^+$ cells in Axin2-rtTA;TetO-H2B-GFP mice. Eight-week-old Axin2-rtTA;TetO-H2B-GFP mice were labelled with doxycycline for 7 days and chased for various lengths of time. Hepatocytes were enzymatically dispersed and sorted by FACS. **a**–**c**, Successive gating shows sequential selection of all hepatocytes (**a**), single cells by forward scatter (**b**), and side scatter (**c**). **d**, Dead cells were excluded by propidium iodide labelling. **e**, GFP-positive cells were gated and either sorted for RNA-seq analysis or further graphed as histograms for GFP intensity analysis (see Fig. 3g).

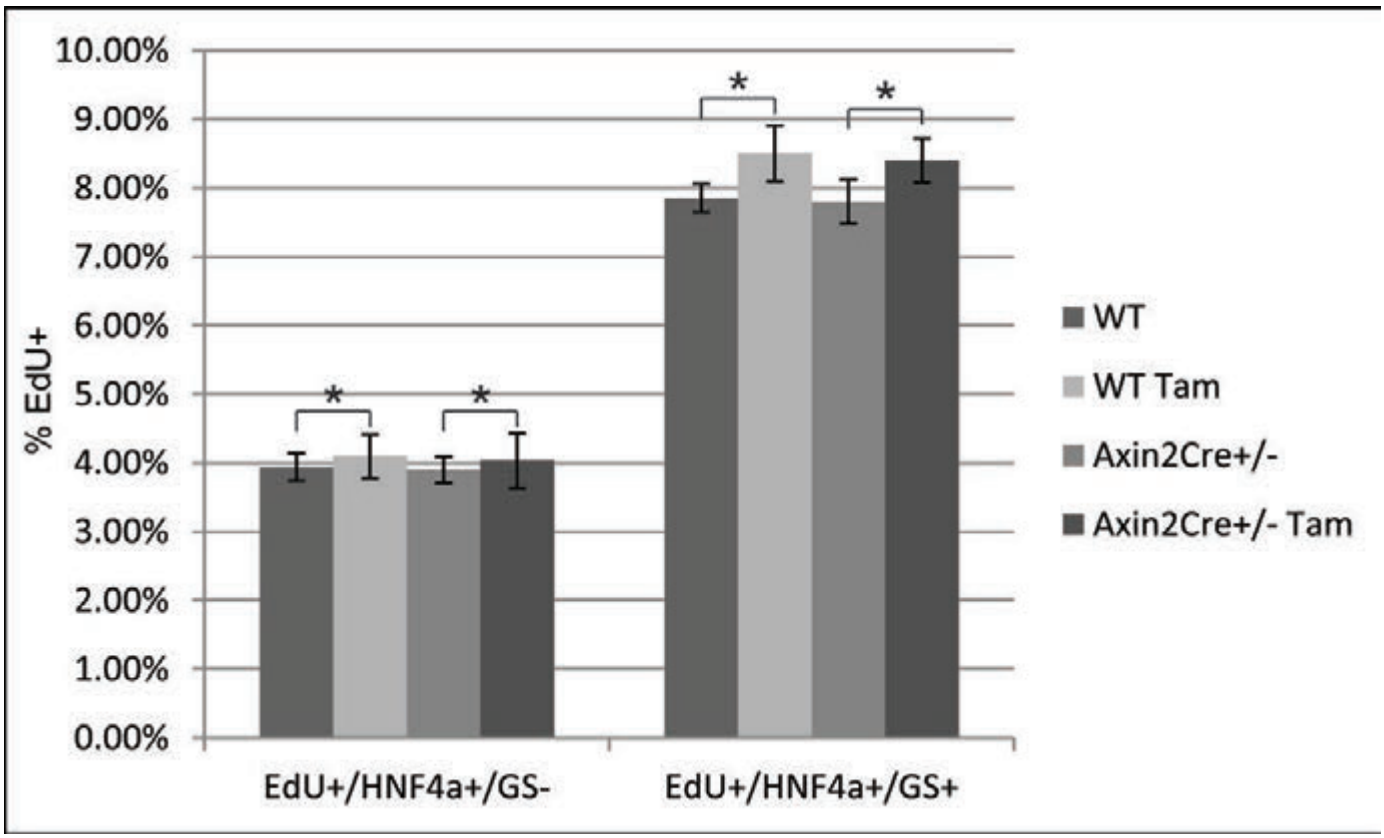

Extended Data Figure 5 | *Axin2* gene dosage and tamoxifen have no effect on pericentral hepatocyte proliferation rate. Wild-type and Axin2CreERT2$^{+/-}$ mice were given EdU daily for 7 days. A subset of wild-type and Axin2CreERT2$^{+/-}$ mice was given 4 mg of tamoxifen per 25 g body weight daily for 5 days. Pericentral hepatocytes were identified by Hnf4a^{+}/GS^{+} staining. All other hepatocytes were identified by Hnf4a^{+}/GS^{-} antibody staining. The EdU-positive rates within the two hepatocyte populations as a percentage of total HNF4a^{+} cells were essentially the same regardless of *Axin2* gene dosage or tamoxifen administration. $n = 5$ animals per group. Data represent mean ± s.e.m. *$P > 0.05$.

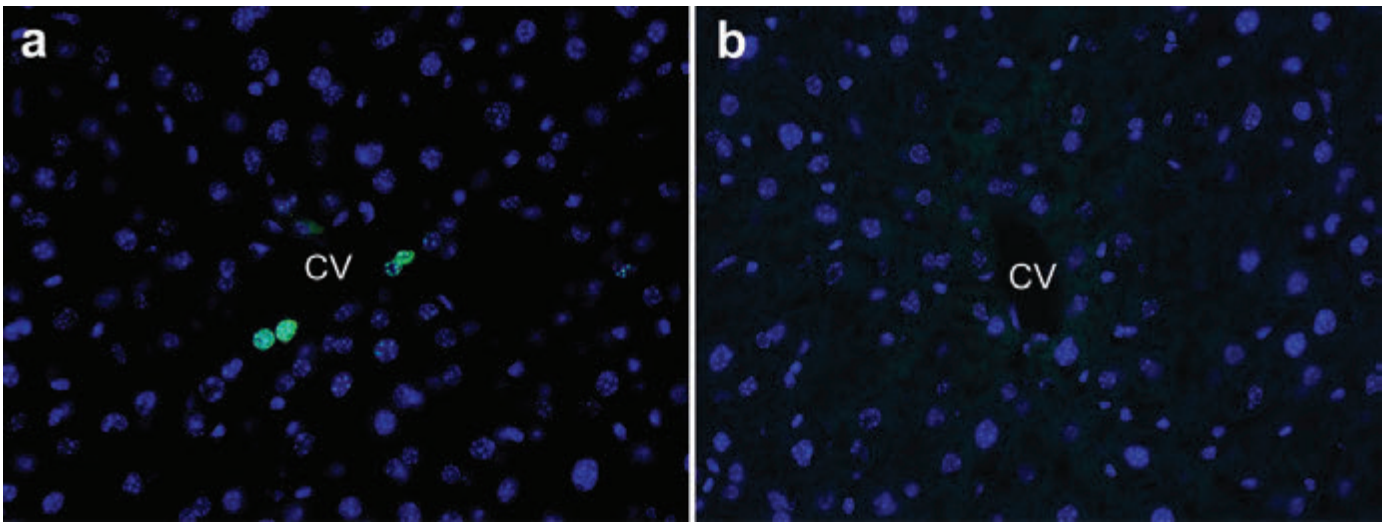

Extended Data Figure 6 | Axin2$^+$ hepatocytes proliferate rapidly. Axin2-rtTA;TetO-H2B-GFP mice were given doxycycline for 7 days. **a**, 56 days after cessation of doxycycline, very few GFP$^+$ cells are seen around the central vein. **b**, After 84 days, no GFP$^+$ cells are seen. Images are representative of $n = 4$ animals per time point.

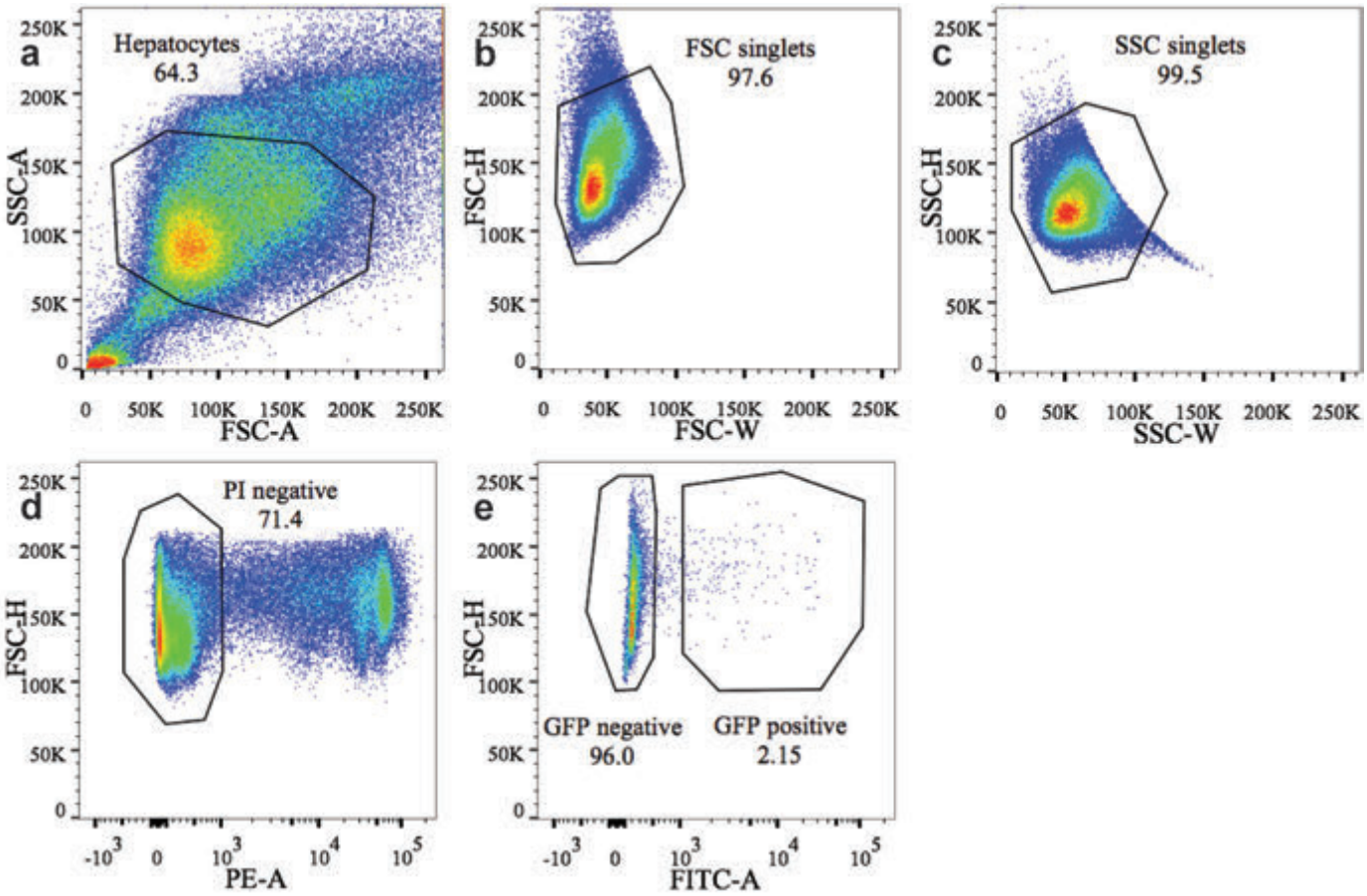

Extended Data Figure 7 | FACS sorting gates for GFP$^+$ cells in Axin2-CreERT2;Rosa26-mTmG^{flox} mice for ploidy analysis. Eight-week-old Axin2-CreERT2;Rosa26-mTmG^{flox} mice were labelled with five daily doses of tamoxifen and traced for 7 days. Hepatocytes were enzymatically dispersed and sorted by FACS. **a**–**c**, Successive gating show sequential selection of all hepatocytes(**a**), single cells by forward scatter(**b**), and side scatter (**c**). **d**, Dead cells were excluded by propidium iodide labelling. **e**, GFP-positive cells were gated and graphed as histograms for Hoechst staining (see Fig. 4).

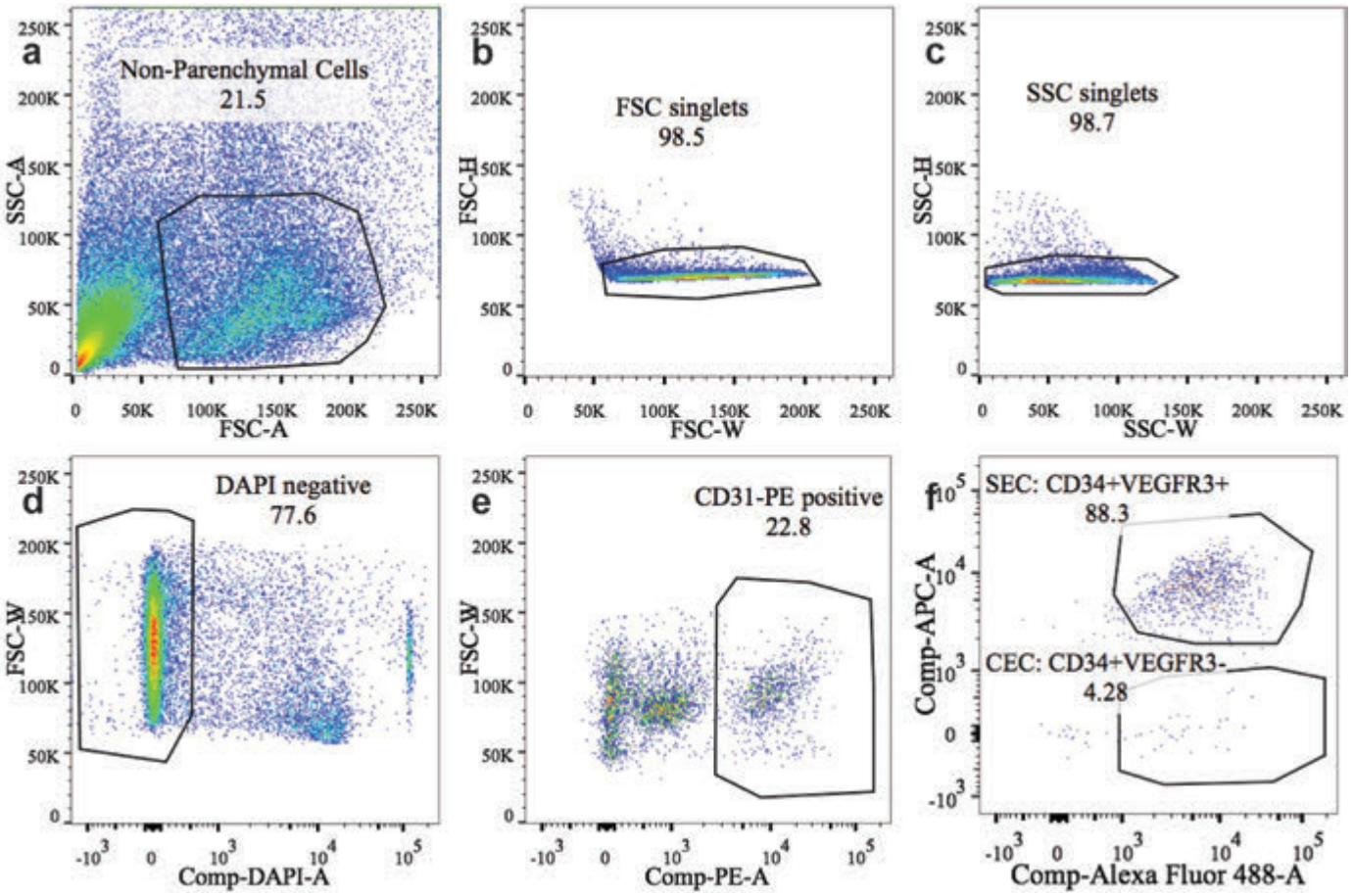

Extended Data Figure 8 | FACS sorting gates for endothelial cells. Eight-week-old wild-type C57B6 mice were used for endothelial cell isolation. Livers were enzymatically digested, hepatocytes were removed by centrifugation and nonparenchymal cells were antibody stained and sorted by FACS. **a**–**c**, Successive gating showed sequential selection of non-parenchymal cells by size (**a**), single cells by forward scatter (**b**), and side scatter (**c**). **d**, Dead cells were excluded by DAPI labelling. **e**, endothelial cells were identified by CD31-phycoerythrin-positive staining. **f**, Sinusoidal endothelial cells (SEC) were identified as CD34-FITC^{+}VEGFR3-APC^{+} while central vein endothelial cells (CEC) were identified as CD34-FITC^{+}VEGFR3-APC^{-}.

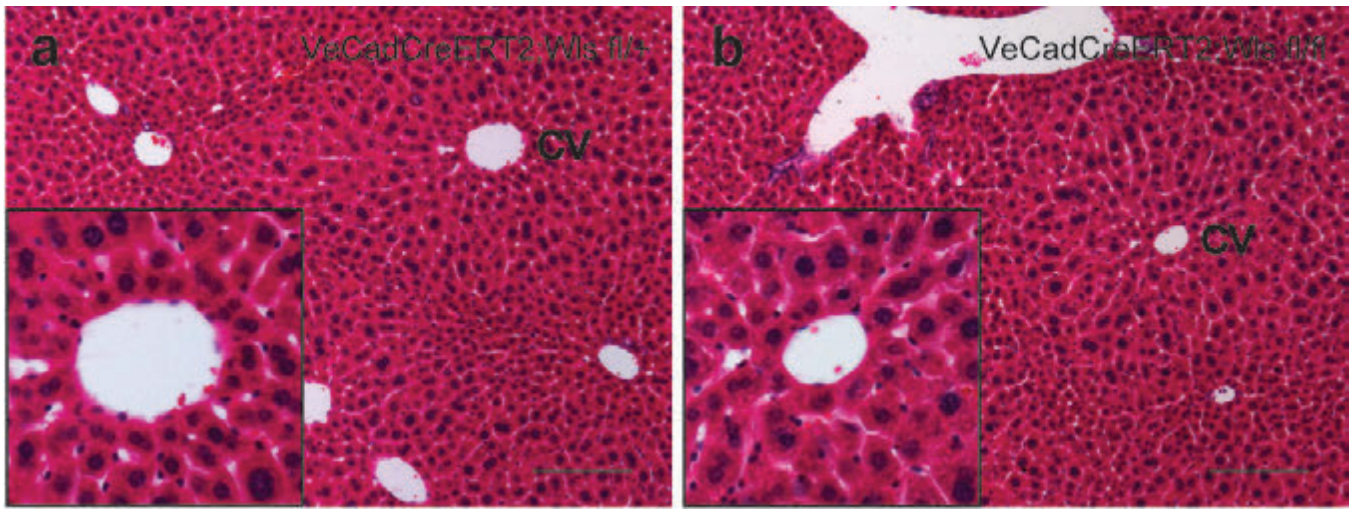

Extended Data Figure 9 | Histology of VE-cadherin-CreERT2;Wls$^{flox/flox}$ animal versus control. **a**, Control (VE-cadherin-CreERT2;Wls$^{flox/+}$) animals given five daily doses of tamoxifen and traced for 7 days after the last tamoxifen dose. Haematoxylin and eosin staining of the liver shows normal histology. **b**, Wls-knockout animals (VE-cadherin-CreERT2;Wls$^{flox/flox}$) also showed normal liver histology. Images are representative images from $n = 5$ animals per group. Insets show central veins. Scale bars, 100 μm.

Extended Data Table 1 | Partial list of differentially expressed genes in Axin2$^+$ vs Axin2$^-$ hepatocytes by RNA-seq analysis

Differentially expressed genes:	Log_2(fold_change):	q-value:
Pericentral:		
Glutamine synthetase (Glul)	-2.58912	0.00961319
Leukocyte cell-derived chemotaxin 2 (Lect2)	-1.85582	0.00961319
Axin2	-1.96625	0.00961319
B glycoprotein (Rhbg)	-3.1865	0.00961319
Cytochrome P450 1a2 (Cyp1a2)	-2.02709	0.00961319
T-box transcription factor 3 (Tbx3)	-1.26286	0.0380302
Periportal:		
Asparaginase (Aspg)	1.25545	0.0441798
Glutaminase 2 (Gls2)	1.53395	0.0441798

Cells were isolated from Axin2-rtTA;TetO-H2B-GFP mice after labelling with doxycycline. Genes preferentially expressed in Axin2$^+$ hepatocytes are indicated by negative log_2 fold changes and genes preferentially expressed in Axin2$^-$ hepatocytes are indicated by positive log_2 fold changes. *q* value (false-discovery-rate-adjusted *P* value) <0.05 used to determine significance.